Metallohelices: Effects of Weak Interactions on Helical Morphology

Tatsuya Kawamoto,[†] Om Prakash,[†] Robert Ostrander,[‡] Arnold L. Rheingold,[‡] and A. S. Borovik*,[†]

Departments of Chemistry, Kansas State University, Manhattan, Kansas 66506, and University of Delaware, Newark, Delaware 19716

Received April 6, 1995

The helix is a dominant structural motif in biomolecules, in which morphology is influenced by noncovalent interactions.[1] Such interactions allow a variety of subtle adjustments in form which are less likely to be achieved with stronger covalent bonds. We are studying synthetic metallohelices which use hydrogen bonds, π-stacking and weak metal−ligand interactions as the predominant forces that determine secondary structure.[2,3] We reason that a reduction in strength of the key structural interactions will render a greater variety of metallohelices which can be used as building blocks to assemble supramolecular species. To test the validity of this approach, we have analyzed the solution and solid state structures for a series of metallohelices of the multidentate ligand 2,6-bis((2-((2-acetylphenyl)-carbamoyl)phenyl)carbamoyl)pyridine, H_2(**1**).[4] Our findings establish that significant morphological variability is obtained for a set of monometallohelices of the same molecular composition and that these differences are amplified in the solid state to yield unique supramolecular species.

H_2(**1**) contains two aryl arrays that are held rigidly through hydrogen bonds and linked covalently to a pyridyl diamide tridentate chelate. The ^{1}H NMR spectrum in $CDCl_3$ of H_2(**1**) shows that the amide protons H_a and H_b have large downfield chemical shifts, indicative of intramolecular hydrogen bonding (Figure 1).[5] These hydrogen bonds restrict the orientation of the aryl rings within the appended arrays as indicated by the strong intraarray NOEs observed between H_b and H_h of the neighboring phenyl ring and between H_l and the methyl protons of the terminal ketone (H_m). In the solid state,[6] H_2(**1**) has a helical structure, which largely results from bifurcated hydrogen bonds between the pyridyl nitrogen, the amide protons (H_a), and the adjacent acyl oxygens (O(2) and O(5)) of the appendages. The appendages cross with a stacking distance of 3.27 Å.

Deprotonation of the pyridyl amides affords a tridentate chelate that becomes planar upon metal ion binding. The acyl oxygens of the appended arrays are predisposed to furnish additional electron density to the metal center. Since these donors are relatively weak Lewis bases, their interactions depend on the stereochemical preference of the bonded metal ion and *not* on the geometric requirements of the ligand.[7] Thus a variety of different helical structures should be obtained either through the binding of different metal ions or by using a metal ion that can accommodate various coordination geometries.[2d,e]

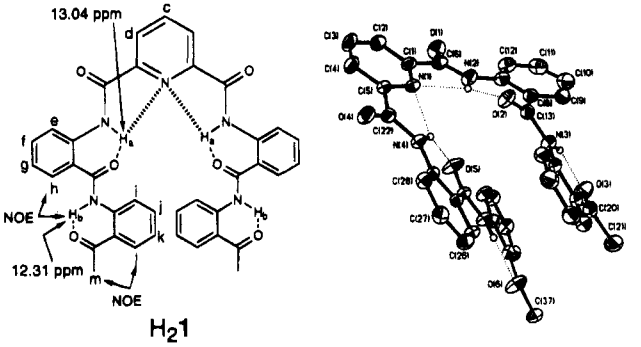

Figure 1. A structural scheme of H_2(**1**) showing selected NMR data (left) and an ORTEP diagram of H_2(**1**) (right) with ellipsoids drawn at the 50% probability level. Non-amide hydrogens are removed for clarity.

The Ni(II) complex of H_2(**1**) (Ni(**1**)) was used to probe whether a metallohelix can be formed in solution.[5,8a] The ^{1}H NMR spectrum of the diamagnetic Ni(**1**) complex ($CDCl_3$) contains one acyl methyl and 10 aryl signals, consistent with a symmetrical coordination of $\mathbf{1}^{2-}$ about the Ni(II) ion.[9] Intramolecular hydrogen bonding within the appended arrays is still present as is evident by the large downfield shift of H_b to 13.01 ppm.[10] Moreover, Ni(**1**) has NOEs analogous to those observed for H_2(**1**). Ni**1** exists as a racemic mixture of left- and right-handed helices which are slow to exchange on the NMR timescale, as demonstrated by treating a $CDCl_3$ solution of Ni(**1**) with [(*S*)-(+)-trifluoro-1-(9-anthryl)ethanol]:[11] an upfield shift and doubling of the proton signals are observed upon addition of this chiral solvating reagent, consistent with the presence of a pair of diastereomeric adducts.[5]

Cu(**1**) allows us to evaluate whether coordination changes at the metal center influence helicity. Recrystallization of Cu(**1**)

* Author to whom correspondence should be addressed.
[†] Kansas State University.
[‡] University of Delaware.

(1) Alber, T. *Prediction of Protein Structure and the Principles of Protein Conformation*; Fasman, G. D.; Ed.; Plenum Press: New York, 1989.
(2) Recent reports of helicates: (a) Lehn, J.-M.; Rigault, A.; Siegel, J.; Harrowfield, J.; Chevier, B.; Moras, D. *Proc. Natl. Acad. Sci. U.S.A.* **1987**, *84*, 2565. (b) Dietrich-Buchecker, C. O.; Sauvage, J.-M. *Angew. Chem., Int. Ed. Engl.* **1989**, *28*, 189. (c) Constable, E. D.; Elder, S. M.; Healy, J.; Ward, M. D.; Tocher, D. A. *J. Am. Chem. Soc.* **1990**, *112*, 4590. (d) Piguet, C.; Bernardinelli, G.; Bocquet, B.; Quattropani, A.; Williams, A. F. *J. Am. Chem. Soc.* **1992**, *114*, 7440. (e) Constable, E. D. *Tetrahedron*, **1992**, *48*, 10013 and references therein. (f) Potts, K. T.; Keshavarz-K, M.; Tham, F. S.; Abruña, H. D.; Arana, C. *Inorg. Chem.* **1993**, *32*, 4436.(g) Bell, T. W.; Jousselin, H. *Nature* **1994**, *367*, 441.
(3) Examples of monometallohelices: (a) Lindoy, L. F.; Busch, D. H.; Goedken, V. *J. Chem. Soc., Chem. Commun.* **1972**, 683. (b) Deuschel-Cornioley, C.; Stoecki-Evans, H.; von Zelewsky, A. *J. Chem. Soc., Chem. Commun.* **1990**, 121. (c) Kawamoto, T.; Kushi, Y. *J. Chem. Soc., Dalton Trans.* **1992**, 3137. (d) Maruoka, K.; Murase, N.; Yamamoto, H. *J. Org. Chem.* **1993**, *58*, 2938.
(4) A paper on the structural chemistry of a molecule nearly identical to H_2(**1**) has recently been published: Hamuro, Y.; Geib, S. J.; Hamilton, A. D. *Angew. Chem. Int. Ed. Engl.* **1994**, *33*, 446.
(5) See supporting information for details.
(6) H_2(**1**): $P\bar{1}$, a = 7.3507(8), b = 10.627(1), and c = 20.098(3) Å; α = 96.64(1), β = 98.07(1), and γ = 90.26(1)°; V = 1543.6(3) Å^3, Z = 2, 3598 unique data ($F_o \geq 4\sigma F_o$), R (R_w) = 0.0523 (0.0656).
(7) Representative papers: (a) Wentworth, R. A. D. *Coord. Chem. Rev.* **1972**, *9*, 172. (b) Wester, D.; Palenik, G. J. *J. Am. Chem. Soc.* **1974**, *96*, 7565
(8) (a) Ni(**1**): IR ν_{CO} 1653 (s), 1635 (s), 1606 (s) cm^{-1}; (b) Cu(**1g**) crystallized with two disordered toluene solvates per molecule: $P\bar{1}$, a = 12.402(3), b = 15.382(3), and c = 23.267(5) Å; α = 107.09(2), β = 90.68(2), and γ = 104.18(2)°; Z = 4, 248 K, 9210 unique data ($F_o \geq 4\sigma F_o$), R (R_w) = 0.0678 (0.0681). (c) Cu(**1r**): $C2/c$, a = 24.087-(6), b = 12.165(3), and c = 23.806 Å; β = 117.450(2)°; 295 K, Z = 8, 2662 unique data ($F_o \geq 4\sigma F_o$), R (R_w) = 0.0411 (0.0486).
(9) This symmetrical coordination in solution is supported by the three carbonyl stretching frequencies observed for Ni(**1**). The frequency for the amide carbonyls of the appendages is similar to that found for hydrogen bonded amides,[10] indicative of weak metal−ligand interactions.
(10) Sorrell, T. N. *Interpreting Spectra of Organic Molecules*; University Science Books: Mill Valley, CA, 1988; p 24.
(11) Pirkle, W. H.; Hoekstra, M. S. *J. Am. Chem. Soc.* **1976**, *98*, 1832.

0020-1669/95/1334-4294$09.00/0

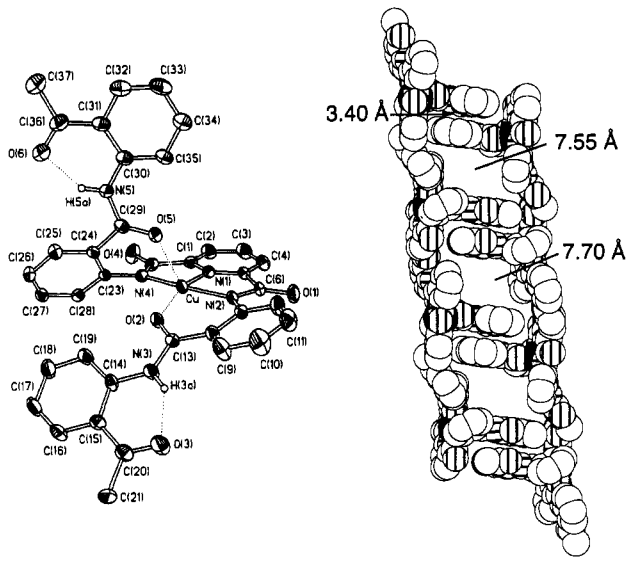

Figure 2. ORTEP diagram of Cu(**1g′**) (left) and space-filling representation (right) for a portion of the crystal lattice in Cu(**1g′**) (view of $b-c$ plane). The solvent molecules and nonamide hydrogens are removed for clarity. Selected distances (Å) and angles (deg): Cu–N(1), 1.904(4); Cu–N(2), 1.967(5); Cu–N(4), 1.965(5); Cu–O(5), 2.315(4); Cu–O(2), 1.931(4); p, 7.613; r, 3.192; ϕ (ϕ'), 0.0 (5.3). Intermolecular aryl–aryl distances are indicated in the figure. Atom key: open circles = carbon; circles with horizontal lines = nitrogen; circles with vertical lines = oxygen; and solid circles = copper.

from toluene/ether affords two crystal types: green and red, both of which have been structurally characterized. The green isomer of Cu(**1**) crystallizes in the centrosymmetric space group $P\bar{1}$ with two crystallographically independent (but virtually identical) molecules (Cu(**1g′**) and Cu(**1g″**); the structure of Cu(**1g′**) is shown in Figure 2.[5,8b] Cu(**1g′**) has a distorted square pyramidal coordination geometry about the copper(II) ion; three nitrogen donors are provided by the rigid pyridyl–diamidate chelate having an average Cu–N_{amide} bond distance of 1.966(5) Å and a Cu–N(1) distance of 1.902(5) Å. Oxygens O(2) and O(5) of the appended arrays bind unsymmetrically to the copper(II) center: the Cu–O(2) distance is 1.931(4), and the of Cu–O(5) distance is 2.315(4) Å. The helical morphology in Cu(**1g′**) results from these unsymmetrical Cu–O_{amide} interactions between the arrays and the metal chelate. For example, the helix in Cu(**1g′**) has a pronounced unsymmetrical twist as is evident by the nonequivalent torsional angles of 0.0 and 5.3° (ϕ and ϕ').[12]

Figure 3 shows the molecular and crystal structures of the red isomer Cu(**1r**).[5,8c] The copper(II) center in Cu(**1r**) is four-coordinate, having Cu–N(1) and Cu–O(2) distances of 1.887(5) and 1.889 (4) Å.

These distances are significantly shorter than those found in Cu(**1g**) and reflect the absence of the weakly coordinated amide O(5) donor in Cu(**1r**). The loss of axial ligation in Cu(**1r**) also results in a major morphological difference in helicity between the two isomers. Since O(5) points away from the copper(II) ion in Cu(**1r**), most of the axially appended array is within van der Waals contacts of the metal chelate; the outer aryl ring of the appendage that contains O(5) is within ~3.60 Å of the plane that contains N(1)–N(2)–N(4). This realignment of the appendage produces a more compact helix compared to those found in the green form. For example, the pitch (p)[12] in Cu-

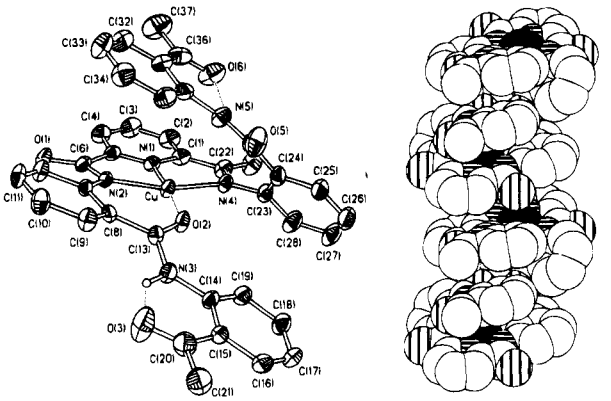

Figure 3. ORTEP diagram of Cu**1r** (left) and space-filling representation (right) for a portion of the crystal lattice in Cu**1r** showing the intermolecular helix (aligned along a-axis). See Figure 2 for atom key. Selected distances (Å) and angles (deg): Cu–N(1), 1.887(5); Cu–N(2), 1.964(4); Cu–N(4), 1.987(4); Cu–O(2), 1.889(4); p, 6.168; r, 2.453; ϕ (ϕ'), −2.8(−1.0).

(**1r**) is smaller by 1.445 Å than that found in Cu(**1g′**) and the radius of the helix (r)[12] has decreased by 0.739 Å.

The differences in structure between the green and red forms of Cu(**1**) are even more pronounced in their crystal lattices. The lattice of Cu(**1g**) is microporous (Figure 2); the pores are formed *via* parallel aryl ring π stacking between the axial appendages of Cu(**1g′**) and Cu(**1g″**) (the aryl–aryl stacking distance is 3.40 Å). The space between adjacent sets of stacked rings (~7.60 Å) contains two disordered toluene molecules. In contrast, the helical molecules of Cu(**1r**) associate to form longer, extended helices in the solid state (Figure 3). Each extended helix consists of alternating right- and left-handed helical monomers that assemble through intermolecular π-stacking interactions. Within an extended helix, two intermolecular Cu–Cu distances (5.504 and 9.131 Å) are observed between a Cu(II) monomer and its nearest neighbors. This close arrangement of molecules in the lattice of Cu(**1r**) yields crystals that are significantly more dense than those found for the porous Cu(**1g**) isomer (Cu(**1r**), 1.505 g/cm^3; Cu(**1g**), 1.137 g/cm^3).[13]

The structural properties of Cu(**1r**) appear to be present only in the crystalline state; dissolution of the red crystals in toluene or CH_2Cl_2 produces green solutions which have spectroscopic properties identical to those found for Cu(**1g**). Nevertheless, these results show that H_2(**1**) and its metal derivatives can produce new and varied helices, and these helices can be used to build supramolecular species that have different structural properties in the solid state. We are currently assessing the applicability of this metal chelate-appendage design in materials having desirable optical or magnetic properties and as nucleators for peptide secondary structure.[14,15]

Acknowledgment is made to the National Science Foundation EPSCoR Program (OSR-9255223) and Kansas State University for financial support of this research.

Supporting Information Available: Text giving spectroscopic analytic data and structure determination summary and tables of X-ray structural data for H_2(**1**), Cu(**1g**), and Cu(**1r**) and ^{1}H NMR spectra of the Pirkle's reagent experiment (38 pages). Ordering information is given on any current masthead page.

IC950397L

(12) Torsional angles (deg): ϕ is described by N(2)–C(7)–C(8)–C(13); ϕ' is described by N(4)–C(23)–C(24)–C(29). Pitch of the helix is the distance (Å) from C(14) to C(30). Radius of helix is the dis-tance (Å) of the line from the Cu(II) center perpendicular to the pitch line.

(13) The lattice of Cu(**1r**) does not contain any solvates.

(14) (a) Lehn, J.-M. *Angew. Chem., Int. Ed. Engl.* **1988**, *27*, 89–112. (b) Constable, E. C. *Angew. Chem., Int. Ed. Engl.* **1991**, *30*, 1450.

(15) Schneider, J. P.; Kelly, J. W. *J. Am. Chem. Soc.* **1995**, *117*, 2533, and references therein.